

# A RAVE investigation on Galactic open clusters

## II. Open cluster pairs, groups and complexes<sup>★</sup>

C. Conrad<sup>1,★★</sup>, R.-D. Scholz<sup>1</sup>, N. V. Kharchenko<sup>1,2,3</sup>, A. E. Piskunov<sup>1,2,4</sup>, S. Röser<sup>2</sup>, E. Schilbach<sup>2</sup>, R. S. de Jong<sup>1</sup>, O. Schnurr<sup>1</sup>, M. Steinmetz<sup>1</sup>, E. K. Grebel<sup>2</sup>, T. Zwitter<sup>5</sup>, O. Bienaymé<sup>6</sup>, J. Bland-Hawthorn<sup>7</sup>, B. K. Gibson<sup>8</sup>, G. Gilmore<sup>9</sup>, G. Kordopatis<sup>1</sup>, A. Kunder<sup>1</sup>, J. F. Navarro<sup>10</sup>, Q. Parker<sup>11</sup>, W. Reid<sup>12</sup>, G. Seabroke<sup>13</sup>, A. Siviero<sup>14</sup>, F. Watson<sup>15</sup>, and R. Wyse<sup>16</sup>

<sup>1</sup> Leibniz-Institut für Astrophysik Potsdam (AIP), An der Sternwarte 16, 14482 Potsdam, Germany  
e-mail: rdscholz@aip.de

<sup>2</sup> Astronomisches Rechen-Institut, Zentrum für Astronomie der Universität Heidelberg, Mönchhofstraße 12–14, 69120 Heidelberg, Germany

<sup>3</sup> Main Astronomical Observatory, 27 Academica Zabolotnogo Str., 03680 Kiev, Ukraine

<sup>4</sup> Russian Academy of Science, Institute of Astronomy, 48 Pyatnitskaya, 109017 Moscow, Russia

<sup>5</sup> Faculty of Mathematics and Physics, University of Ljubljana, Jadranska 19, 1000 Ljubljana, Slovenia

<sup>6</sup> Observatoire astronomique de Strasbourg, Université de Strasbourg, CNRS, UMR 7550, 11 rue de l'Université, 67000 Strasbourg, France

<sup>7</sup> Sydney Institute for Astronomy, School of Physics A28, University of Sydney, NSW 2006, Australia

<sup>8</sup> Centre for Astrophysics, Department of Physics and Mathematics, University of Hull, Hull, HU6 7RX, UK

<sup>9</sup> Institute of Astronomy, Cambridge University, Madingley Road, Cambridge CB3 0HA, UK

<sup>10</sup> Department of Physics and Astronomy, University of Victoria, Victoria, BC V8P5C2, Canada

<sup>11</sup> Department of Physics, Laboratory for Space Research, University of Hong Kong, Cyberport 4, 100 Cyberport Rd, Telegraph Bay, Hong Kong, PR China

<sup>12</sup> Department of Physics and Astronomy, Macquarie University, Sydney, NSW 2109, Australia

<sup>13</sup> Mullard Space Science Laboratory, University College London, Holmbury St Mary, Dorking, RH5 6NT, UK

<sup>14</sup> Dipartimento di Fisica e Astronomia Galileo Galilei, Università di Padova, Vicolo dell'Osservatorio 3, 35122 Padova, Italy

<sup>15</sup> Australian Astronomical Observatory, PO Box 915, North Ryde, NSW 1670, Australia

<sup>16</sup> Johns Hopkins University, Dept of Physics and Astronomy, Baltimore, MD 21218, USA

Received 4 November 2016 / Accepted 15 December 2016

### ABSTRACT

**Context.** It is generally agreed upon that stars form in open clusters (OCs) and stellar associations, but little is known about structures in the Galactic OC population; whether OCs and stellar associations are born isolated or if they prefer to form in groups, for example. Answering this question provides new insight into star and cluster formation, along with a better understanding of Galactic structures. **Aims.** In the past decade, studies of OC groupings have either been based solely on spatial criteria or have also included tangential velocities for identifications. In contrast to previous approaches, we assumed that real OC groupings occupy a well defined area in the sky and show similar velocity vectors. For the first time, we have used 6D phase-space information, including radial velocities from the RAdial Velocity Experiment (RAVE) and other catalogues, for the detection of OC groupings. We also checked the age spread of potential candidates to distinguish between genuine groupings and chance alignments.

**Methods.** We explored the Catalogue of Open Cluster Data (COCD) and determined 6D phase-space information for 432 out of 650 listed OCs and compact associations. The group identification was performed using an adapted version of the Friends-of-Friends algorithm, as used in cosmology, with linking lengths of 100 pc and 10–20 km s<sup>-1</sup>. For the verification of the identified structures, we applied Monte Carlo simulations with randomised samples.

**Results.** For the linking lengths 100 pc and 10 km s<sup>-1</sup>, we detected 19 groupings, including 14 pairs, 4 groups with 3–5 members, and 1 complex with 15 members. The Monte Carlo simulations revealed that, in particular, the complex is most likely genuine, whereas pairs are more likely chance alignments. A closer look at the age spread of the complex and the comparison between spatial distributions of young and old cluster populations suggested that OC groupings likely originated from a common molecular cloud.

**Key words.** open clusters and associations: general – stars: kinematics and dynamics – Galaxy: kinematics and dynamics – stars: abundances – solar neighborhood

### 1. Introduction

Star formation is believed to take place in a clustered mode (Lada & Lada 2003; Lada 2006) and also galaxies tend to form in groups (Kravtsov & Borgani 2012; Demiański & Doroshkevich 2014). We are interested in knowing whether or not this is also the case for open clusters; more specifically, whether stellar clusters preferably form isolated or in a clustered mode.

\* Tables A.1, A.2, and B.1 are only available at the CDS via anonymous ftp to [cdsarc.u-strasbg.fr](http://cdsarc.u-strasbg.fr) (130.79.128.5) or via <http://cdsarc.u-strasbg.fr/viz-bin/qcat?J/A+A/600/A106>  
\*\* Current postal address: Elfenstraße 43, 68169 Mannheim, Germany.

Until now open clusters (OCs) have mainly been investigated as isolated stellar systems. Investigations of groupings of Galactic OCs shed new light on the formation of stars and help to better understand the structure and dynamics of our Milky Way. Piskunov et al. (2006) found accumulations of objects in the Catalogue of Open Cluster Data (COCD; Kharchenko et al. 2005a,b) based on spatial distributions and tangential velocities, after they divided their sample into age bins. In analogy with star-forming complexes containing associations and young clusters, Piskunov et al. (2006) defined open cluster complexes (OCCs) as large physical aggregates of (classical) OCs, “identified by a sufficient amount of data”. Smaller cluster formations, with only “fragmentary data available”, were referred to as OC groups. They proposed two groups, namely the Perseus-Auriga group with eight members of ages between 220 and 400 Myr and the Hyades moving group with nine members of ages between 0.4 and 1.4 Gyr. The OCCs proposed by Piskunov et al. (2006) are younger: OCC1 with 21 members covers an age range from 5 to 50 Myr and OCC2 harbours 21 members of ages between 204 and 390 Myr. In our own work, we define OC groupings as cluster pairs (2), groups (3–10) and complexes (>10) simply based on the number of members.

de la Fuente Marcos & de la Fuente Marcos (2009a,b,c) provided a series of papers on primarily pairs of OCs based on the WEBDA online database<sup>1</sup> (created by Mermilliod (1988) and maintained by Netopil et al. (2012)) and the New Optically Visible Open Clusters and Candidates catalog<sup>2</sup> (Dias et al. 2002, hereafter DAML). In their first paper, de la Fuente Marcos & de la Fuente Marcos (2009a) focused on the investigation of a kinematically coherent OC group spread over the Cassiopeia and Perseus constellations. This Cassiopeia-Perseus family is located at a distance of approximately 2 kpc with a diameter of 600 pc and the members cover an age range of 20–40 Myr. In their second publication, de la Fuente Marcos & de la Fuente Marcos (2009b) assumed that the separation of OC pairs should not exceed three times the typical cluster tidal radius ( $\sim 30$  pc) in the Milky Way. Due to incompleteness at higher distances, they split up their sample. Within their volume-limited sample ( $d < 850$  pc), they identified 16 pairs, two triples and one quadruple. At higher distances, they found 18 additional OC pairs and one more triple with distances up to 2.3 kpc. In their third paper, de la Fuente Marcos & de la Fuente Marcos (2009c) discussed the hierarchy of star formation in the Galactic disc based on OC pairs. They found evidence for highly hierarchical star formation in the Milky Way and stated that in neighbouring regions, star formation is synchronised. This limits the time interval available for cluster formation and de la Fuente Marcos & de la Fuente Marcos (2009c) concluded that the vast majority of clusters form in larger complexes.

In the Milky Way, Piatti et al. (2010) verified another binary of OCs with a separation of 3.6 pc. Both these clusters are rather small with individual total radii of approximately 1 pc. Elias et al. (2009) investigated the Gould belt OC population and found differences between the Orion and Sco-Cen regions. The former showed a very clumpy structure and can, therefore, be referred to as a cluster complex. The latter seemed to be dominated by isolated star formation and is more likely an OB association. Elmegreen (2009, 2011) supported the picture of hierarchical star formation in the Milky Way. They found that the fragmentation of giant molecular clouds is reflected in the distribution of

young stars. On the largest scale, they form cluster complexes, and on smaller scales, they are found to form OB associations and OCs down to isolated stars.

In addition to the Galactic studies, there were a number of investigations on hierarchical star formation in nearby galaxies. Elmegreen & Efremov (1996) analysed the hierarchy not only in the Milky Way, but also in the Large Magellanic Cloud (LMC). Bonatto & Bica (2010) investigated the Magellanic Clouds and identified similar patterns as in the Milky Way. For example that the young stars followed the fragmentation of the gas. Moreover, the degree of grouping appeared to be higher for young clusters than for old ones, which they suggested to be most likely caused by dynamical interactions. Dieball et al. (2002) investigated the distribution of young populous clusters in the Magellanic clouds, concentrating on the LMC. They searched for binary and multiple clusters with a maximum separation of approximately 20 pc. Based on a statistical analysis, they found that, depending on region, 12 (outer LMC) to 56% (bar region) of the pairs are probably genuine. For the cluster binaries and multiples with available ages, they found that the multiples are usually younger. They conclude that most of the cluster pairs and groups formed from a common molecular cloud and not through capture.

In M33, the fractal dimension of molecular gas was found to be significantly smaller than for the Milky Way (Sánchez et al. 2010) with a transition from fractal structures to uniform distributions at a scale of approximately 500–1000 pc. Efremov (2010) and Gusev & Efremov (2013) investigated star-cluster complexes in the spiral arms of M31 and M74, respectively. For both galaxies, the cluster complexes appeared to be almost equally spaced in a chain-like structure along the spiral arms. In the framework of the LEGUS project (Legacy ExtraGalactic UV Survey; Calzetti et al. 2015) with HST, several studies on the distribution of young massive clusters in a variety of nearby star-forming galaxies were conducted. In their sample of 12 late-type galaxies, Elmegreen et al. (2014) found hierarchically structured star-forming regions the size of a few hundred pc, supporting the existence of cluster groups. Gouliermis et al. (2015) focused on NGC 6503 and verified hierarchical structures in the star-forming ring, while Grasha et al. (2015) found that in the NGC 628 galaxy, the clustering of young stellar clusters decreases with cluster age. These findings suggest that OC groupings exist in galaxies other than our own.

## 2. The data

### 2.1. The catalogues

This work is primarily based on the COCD defining a homogeneous sample of 650 Galactic OCs and compact associations. Since there are only seven compact associations among the 650 entries in the COCD, we refer to all objects as OCs or clusters. In addition to the overall OC values in the COCD, Kharchenko et al. (2004, 2005b) provide stellar catalogues (CSOCA) containing individual information on each star in the area around the investigated clusters. For each star, they list membership probabilities ( $P$ ) based on kinematics, photometry and spatial distribution. The most probable members are called  $1\sigma$ -members, with  $P_{\text{kin}}$  and  $P_{\text{phot}} > 61\%$ , while probable members are referred to as  $2\sigma$ -members, with  $P_{\text{kin}}$  and  $P_{\text{phot}} > 14\%$ , and the least possible members with  $P_{\text{kin}}$  and  $P_{\text{phot}} > 1\%$  are called  $3\sigma$ -members. The Catalogue of Radial Velocities with Astrometric Data (CRVAD-2; Kharchenko et al. 2007) provided a source for updating the radial velocity (RV) information in the CSOCA. Newly determined RVs for OCs were

<sup>1</sup> WEBDA – <http://www.univie.ac.at/webda>

<sup>2</sup> DAML – <http://www.astro.iag.usp.br/~wilton/>

summarised in the Catalogue of Radial Velocities of Open Clusters and Associations (CRVOCA; Kharchenko et al. 2007).

Furthermore, we took advantage of a special observing program of 85 COCD clusters in the Galactic plane initiated within the RAdial Velocity Experiment (RAVE; Steinmetz et al. 2006) and cross-matched the stars in all 650 COCD areas with the RAVE fourth data release (DR4; Kordopatis et al. 2013) to obtain additional RV values on cluster members. Recently, RAVE came out with data release five (DR5; Kunder et al. 2017), but as RAVE DR5 includes very few new stars in OCs listed in the COCD and because the RV determination in DR5 was essentially unchanged from DR4, the use of DR5 instead of DR4 will not change our conclusions. The sample was cleaned using quality constraints and flags, as well as membership probabilities (Conrad et al. 2014, hereafter referred to as Paper I). With RAVE, we were able to measure mean RVs of 110 COCD clusters, including 37 OCs, for which no previous measurements were available.

## 2.2. Parameters

In Paper I, we showed that the CRVAD-2 and RAVE provide RV data of similar quality, which allowed us to combine the measurements from both catalogues and recompute the mean RVs for 432 COCD clusters. If a star had multiple RV measurements in RAVE, we took the value derived from the spectrum with the higher Signal-to-Noise ratio (SNR). If a cluster showed no individual RV measurements of sufficient quality in CRVAD-2 or RAVE, we used the RV value listed in CRVOCA. Though we gained more RV data for the clusters through combining the CRVAD-2 and RAVE data sets, the mean cluster RVs are mainly based on less than seven individual measurements and still suffer from small number statistics. The uncertainties for the cluster RV showed a similar distribution as presented in Paper I, that is, they peak at approximately  $1\text{--}2\text{ km s}^{-1}$  with a tail out to  $20\text{ km s}^{-1}$ . This confirmed that the RV data quality is of sufficient quality for the purpose of our population investigation.

Besides RVs we also needed distances, ages and proper motions, which were taken from the COCD, mainly because these parameters were available for all COCD entries. The distances in the COCD were derived from two-colour information and spectral type information, where available. If this information was not available, we used listed literature values from Kharchenko et al. (2005a,b). In addition, they stated that the distances were accurate to the 10% level. The cluster ages in the COCD were obtained from isochrone fitting or taken from the literature with a stated general uncertainty of  $\sigma_{\log t} = 0.2\text{--}0.25$  dex (for details see Kharchenko et al. 2005a,b).

The proper motions (PMs) in the COCD were provided in the equatorial system ( $\text{PM}_{\text{RA}}$  and  $\text{PM}_{\text{Dec}}$ ) as well as in the Galactic coordinate system ( $\text{PM}_l$  and  $\text{PM}_b$ ) and based on values from the All-Sky Compiled Catalogue of 2.5 million stars (ASCC-2.5; Kharchenko 2001). However, uncertainties were only provided in the equatorial coordinate system and are mainly below  $1\text{ mas/yr}$ . Their distribution is illustrated in Fig. 1. For the uncertainties of the proper motions in the Galactic system we assumed that  $e\text{PM}_l \approx e\text{PM}_b = e\text{PM}_{\text{gal}}$  with

$$e\text{PM}_{\text{gal}} = \sqrt{\frac{e\text{PM}_{\text{RA}}^2 + e\text{PM}_{\text{Dec}}^2}{2}}.$$

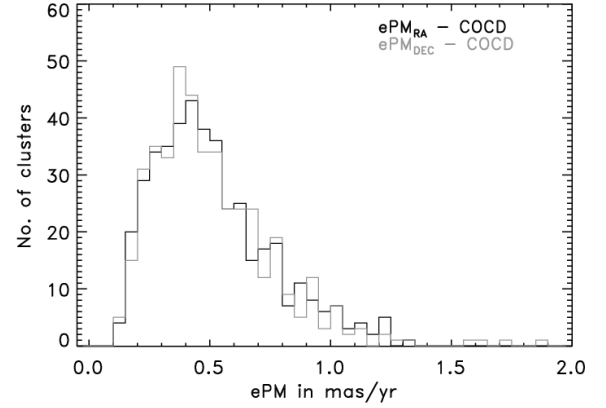


Fig. 1. Histograms for the  $e\text{PM}_{\text{RA}}$  (black) and  $e\text{PM}_{\text{Dec}}$  (grey) for the clusters in the working sample.

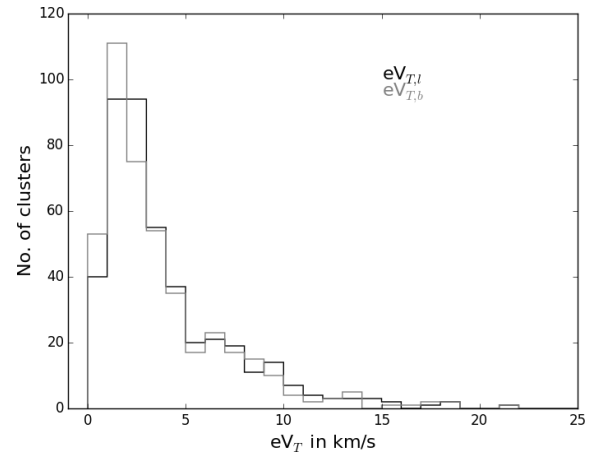


Fig. 2. Histogram for uncertainties in  $V_T$  in Galactic longitude ( $l$ , black) and latitude ( $b$ , grey) for the clusters in our working sample.

For computing Cartesian coordinates, we transformed the PM values to tangential velocities using Eq. (2)

$$V_T = kd \cdot \text{PM}, \quad (1)$$

$$eV_T = k \sqrt{[(d \cdot e\text{PM})^2 + (ed \cdot \text{PM})^2]}, \quad (2)$$

where  $V_T$  is the tangential velocity component of interest in  $\text{km s}^{-1}$ ,  $k = 4.74$  is a factor ensuring unit consistency, PM the proper motion component of interest in  $\text{mas/yr}$ , and  $d$  the distance of the cluster to the Sun in kpc.

The distributions for the resulting uncertainties ( $eV_T$ ) in the Galactic coordinate system are displayed in Fig. 2. The tangential velocity uncertainties, which are dominated by the distance uncertainties, are comparable to (slightly larger than) the RV uncertainties. The cluster  $eV_T$  peak at approximately  $2\text{--}3\text{ km s}^{-1}$ , while the cluster  $e\text{RV}$  values peak at approximately  $1\text{--}2\text{ km s}^{-1}$  and the tail of the  $eV_T$  distribution reaches slightly beyond  $20\text{ km s}^{-1}$ , while all  $e\text{RV}$  are below  $20\text{ km s}^{-1}$ . All basic parameters for the 432 clusters in our working sample are summarised in Table A.1.

Metallicities are only available for approximately 30% of the working sample and are relatively inhomogeneous. This is because different instruments and techniques were used to determine the metallicities for the individual clusters. Therefore, we will not use them for a detailed analysis or evaluation of the possibly identified OC groupings. However, for completeness, the summarising tables are available at the CDS.

### 2.3. 6D phase-space information

The parameters presented in the previous section were then used to compute Cartesian coordinates, which are more convenient for identifying OC groupings. The  $XYZ$ -coordinates were obtained from a conversion of spherical Galactic coordinates to Cartesian coordinates following Eq. (3), where  $l$  and  $b$  are the Galactic longitude and latitude in degrees and  $d$  is the distance of the cluster to the Sun in kpc. In this work, the positive  $X$ -axis points towards the Galactic anticentre, the  $Y$ -axis is positive in direction of Galactic rotation and the positive  $Z$ -axis points towards the north Galactic pole.

$$\begin{pmatrix} X \\ Y \\ Z \end{pmatrix} = \begin{pmatrix} -d(\cos b \cos l) \\ d(\cos b \sin l) \\ d \sin b \end{pmatrix}. \quad (3)$$

The  $UVW$ -velocities were converted from the spherical values in the Galactic coordinate system, but we had to correct the RV and PM values for differential rotation beforehand (see Eqs. (4)–(6)). For Eqs. (4)–(6) we adopted Oort’s linear model for the differential Galactic rotation in the vicinity of the Sun. The parameters  $(A, B) = (14.5, -13) \text{ km s}^{-1} \text{ kpc}^{-1}$  in Eqs. (4)–(6) are the Oort constants as determined by Piskunov et al. (2006) for the Galactic OC population in the COCD.

$$RV_{\text{corr}} = RV - Ad \sin 2l \cos b^2. \quad (4)$$

$$PM_{l,\text{corr}} = PM_l - ([A \cos 2l + B] \cos b/k). \quad (5)$$

$$PM_{b,\text{corr}} = PM_b + ([A \sin 2l \sin 2b]/2k). \quad (6)$$

The Galactic  $UVW$ -velocities were then computed using Eq. (7), with  $U$  being positive towards the Galactic anticentre,  $V$  positive in direction of Galactic rotation and  $W$  being positive towards the north Galactic pole. The correction for the solar motion was applied in the final equation through simply adding the values provided by Piskunov et al. (2006) for the Galactic OC population:  $(U_0, V_0, W_0) = (-9.44, 11.9, 7.2) \text{ km s}^{-1}$ . The change of sign in  $U_0$  between Piskunov et al. (2006) and this work is because of the flipped direction of the  $X$ -axis.

$$\begin{pmatrix} U \\ V \\ W \end{pmatrix} = 4.74d \left[ PM_{l,\text{corr}} \begin{pmatrix} -\sin l \\ \cos l \\ 0 \end{pmatrix} + PM_{b,\text{corr}} \begin{pmatrix} -\cos l \sin b \\ -\sin l \sin b \\ \cos b \end{pmatrix} \right] + RV_{\text{corr}} \begin{pmatrix} \cos l \cos b \\ \sin l \cos b \\ \sin b \end{pmatrix} + \begin{pmatrix} U_0 \\ V_0 \\ W_0 \end{pmatrix}. \quad (7)$$

These  $UVW$ -velocities are computed with respect to the centroid of the OC system (Piskunov et al. 2006).

A brief look at the  $UVW$ -uncertainties (Fig. 3), as calculated following Gaussian error propagation, showed that they cover a similar range as the uncertainties of the input velocities ( $RV$  and  $V_T$ ). For all components, the uncertainties peak at approximately 2–4  $\text{km s}^{-1}$  and the vast majority of values are well below 20  $\text{km s}^{-1}$ . This confirms that the  $UVW$ -velocities are of sufficient accuracy for the purpose of this project. All computed Cartesian parameters for the 432 clusters in our working sample are summarised in Table A.2, along with ages and available metallicity information.

## 3. Galactic OC groupings

### 3.1. Identification of OC groupings

Members of an OC grouping are expected to show spatial proximity. If the number of such groupings is large enough, they appear as an additional peak in the separation distribution for the

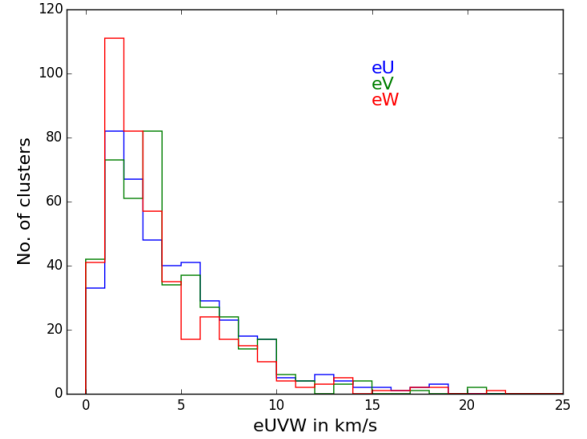


**Fig. 3.** Histograms for the uncertainties in the computed and corrected Cartesian velocities ( $U$  – blue,  $V$  – green,  $W$  – red) in our OC working sample.

nearest neighbours (upper panel of Fig. 4). Furthermore, members of an OC grouping should have similar velocity vectors. In general, objects in a restrained area of the Galactic disc are expected to move in a similar direction at comparable speeds with a velocity dispersion indicating the amount of random motion in that region. For the purpose of this investigation, we evaluated this random motion to gain further insight into the importance of including velocities in the identification algorithm.

The middle panel of Fig. 4 shows the histogram for the minimal velocity difference between OC pairs, regardless of spatial proximity. This distribution most likely reflects the velocity dispersion of the Galactic disc in the solar vicinity. The lower panel of Fig. 4 illustrates the histogram for the velocity difference between a cluster and its nearest spatial neighbour. It is interesting that the latter distribution is much broader than the one for the minimal velocity difference, which verified the necessity for including the velocity vector for the group identification. Moreover, the difference between the distributions in the middle and lower panels of Fig. 4 show that there is a non-negligible amount of random motion present in the Galactic OC population.

A relatively simple tool to identify clumps or groups in populations is the Friends-of-Friends (FoF) algorithm, as used in cosmology (Huchra & Geller 1982; Geller & Huchra 1983). The basic working principle is the search for potential neighbours around each object in a population within a predefined search radius, the so called linking length. This linking length is basically the maximum separation of members belonging to a clump or group and is typically a fraction of the average separation of objects in the considered population. In this study, we applied an adaption of this FoF algorithm in coordinate and velocity space, since we requested that members of an OC grouping occupy a well defined region in space and show similar velocity vectors at the same time. To define the linking lengths in coordinate and velocity space, we considered the 3D-spatial separation and 3D-velocity difference.

The spatial linking length should have a value between the typical size of OCs (tidal radius of 1–70 pc; Kharchenko et al. 2009) and the scale of the Galactic spiral arms (width  $\approx 1$  kpc). The OC pairs identified by de la Fuente Marcos & de la Fuente Marcos (2009b) were selected based on the assumption that the separation should be below 30 pc, while the OC groups and complexes proposed by Piskunov et al. (2006) span regions of approximately 300 pc. The separation histogram for the nearest neighbours in our

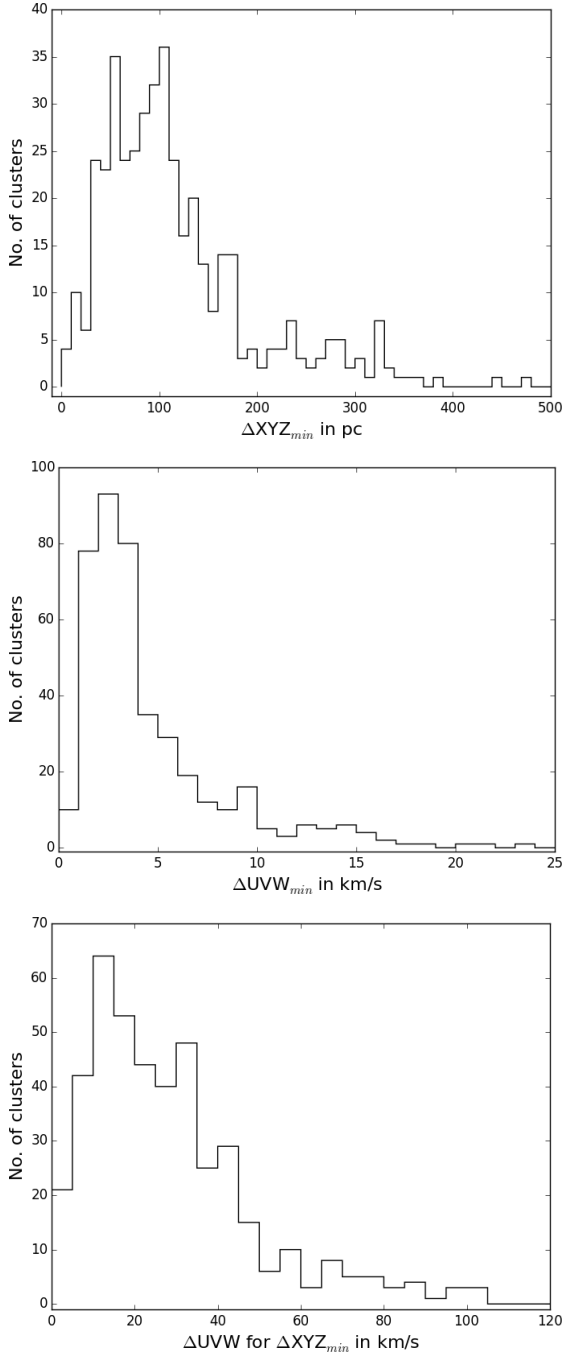


**Fig. 4.** Histograms for the spatial separation of the nearest neighbours in  $XYZ$ -space (*upper panel*), as well as for the velocity differences of nearest neighbours in  $UVW$ -space (*middle panel*), regardless of spatial proximity, and velocity difference between the nearest neighbours in  $XYZ$ -space (*lower panel*).

working sample shows two peaks at approximately 50 and 100 pc (upper panel of Fig. 4), which might be a signature for OC groupings. Thus, setting the spatial linking length in the FoF-like algorithm to 100 pc is a reasonable choice, although it retains the possibility that the groups and complexes proposed by Piskunov et al. (2006) may not be recovered in their entirety.

The velocity linking length should be comparable to a few multiples of the typical internal velocity dispersion of OCs. For very young OCs in the Infrared Spectroscopy of Young Nebulous Clusters program (IN-SYNC) within the third Sloan Digital Sky Survey (SDSS-III), with ages of 1–2 Myr, internal

velocity dispersions of approximately  $1 \text{ km s}^{-1}$  were detected (Cottaar et al. 2014; Foster et al. 2015). Theoretical studies by Bate (2009) and Bate (2012) found values of 3–5  $\text{km s}^{-1}$  for the internal velocity dispersion of OCs.

The  $UVW$ -uncertainties were typically 3–4  $\text{km s}^{-1}$  and mostly below 20  $\text{km s}^{-1}$  (see Fig. 3), but show a rather broad distribution. Since the distribution for the  $UVW$ -uncertainties exceeds the expected values for the OC velocity dispersion, we prefer to use the former to define the velocity linking length. The typical  $UVW$ -uncertainties are well below 10  $\text{km s}^{-1}$ , but the distribution continues to values of 20  $\text{km s}^{-1}$ . Thus, it is more reasonable to define the range of 10–20  $\text{km s}^{-1}$  for the velocity linking length than a single value and we ran the FoF-like algorithm twice: firstly, with 100 pc and 10  $\text{km s}^{-1}$  and secondly, with 100 pc and 20  $\text{km s}^{-1}$ .

The resulting distributions in coordinate and velocity space of the identified groupings are displayed in the upper and lower panels of Fig. 5, respectively. In this study, we distinguish between pairs (two members), groups ( $\leq 10$  members) and complexes ( $> 10$  members) of OCs. Interestingly, the majority of identified groupings are pairs for both sets of linking lengths. The identified OC groupings are preferably detected in the immediate solar neighbourhood at  $\approx 1$  kpc for a velocity linking length of 10  $\text{km s}^{-1}$  and within  $\approx 2$  kpc for 20  $\text{km s}^{-1}$ . In velocity space, the distribution of identified OC groupings appears to be less centralised than in coordinate space and the groupings do not separate as clearly upon visual inspection.

As expected, the number and size of the identified OC groupings increases with larger velocity linking length. At a velocity linking length of 10  $\text{km s}^{-1}$ , we found, in total, 19 groupings with 14 pairs, 4 groups with 3, 4 or 5 members, and 1 complex with 15 members (left panel of Fig. 6). At a velocity linking length of 20  $\text{km s}^{-1}$ , we identified, in total, 41 groupings with 31 pairs, 9 groups with 3 to 9 members, and 1 complex with the same 15 members (right panel of Fig. 6).

A closer look at the upper panels of Fig. 5 shows that there are not only more and larger groupings after increasing the velocity linking length, but that some smaller groupings seem to merge, for example at  $X \approx 0$  kpc and  $Y \approx -0.1$  kpc or  $X \approx 0.2$  kpc and  $Y \approx -0.4$ . Still, the number and size of the identified OC groupings remained reasonable for the chosen range of velocity linking lengths. Based on previous studies, it is expected that only a fraction of clusters are members of groups. It is unlikely that all clusters are part of groupings, as the cluster ages in the sample reaches up to a few Gyr, where the majority of cluster groupings have already dissolved. Moreover, pairs or small number multiples are more likely than complexes with a lot of members. This is supported by the values in Table B.1, summarising the members and mean parameters for the detected groupings for both sets of linking lengths, including metallicity information where available.

### 3.2. Verification of OC groupings

Though the definition of the linking lengths for the OC grouping identification algorithm is based on reasonable assumptions, the linking lengths are, to a certain degree, arbitrary. Hence, it is recommended to conduct further verification of the structures found to verify our findings. Therefore, we carried out Monte Carlo simulations with randomised data sets. Since all potential groupings for either set of linking lengths are located within 2 kpc, we implemented the simulations within a sphere of 1.8 kpc, ensured by the criterion  $\sqrt{X^2 + Y^2 + Z^2} \leq 1.8$  kpc. Within this region,

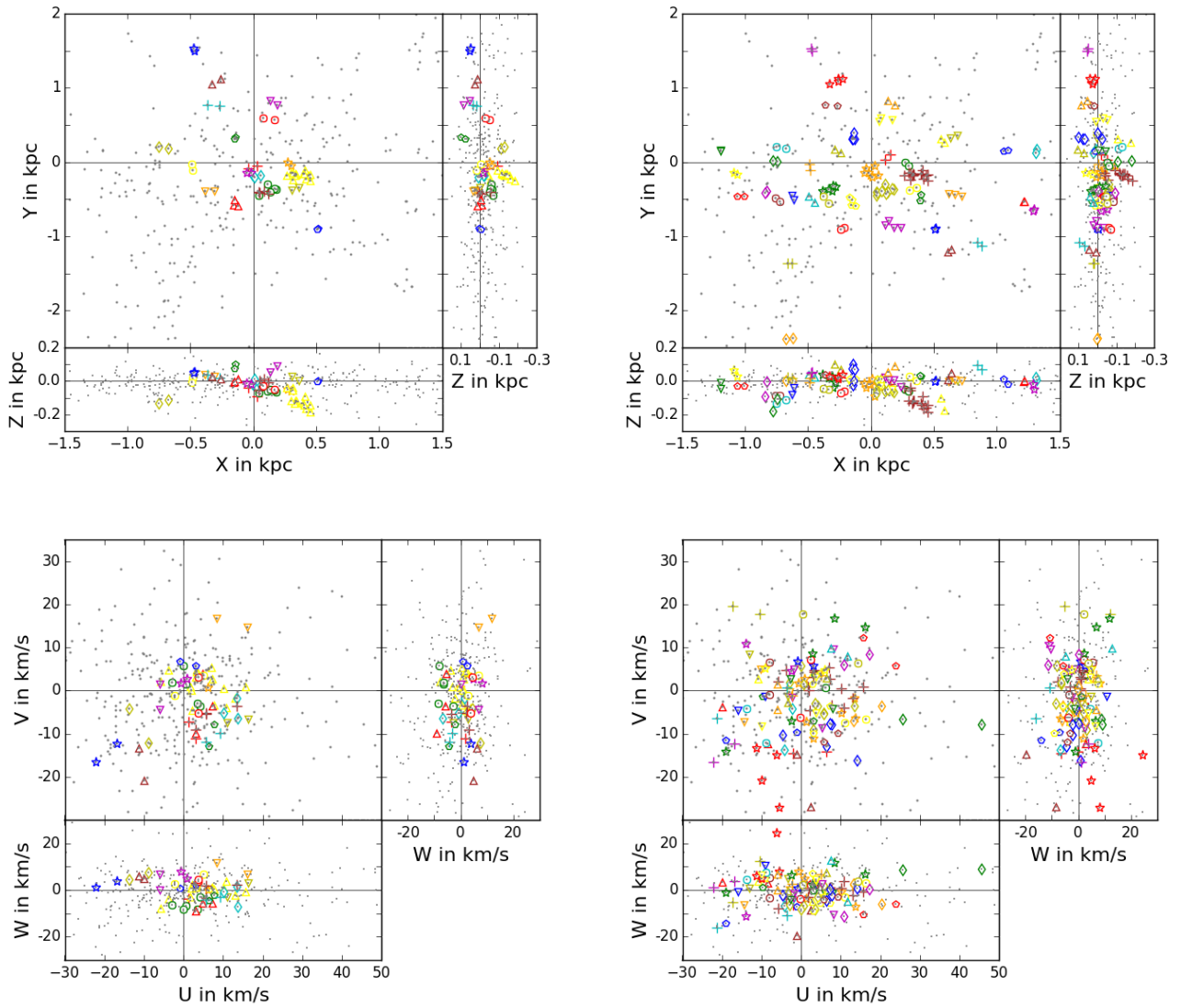


**Fig. 5.** Distribution of the identified OC groupings in coordinate (*upper panels*) and velocity (*lower panels*) space for a spatial linking length of 100 pc and a velocity linking length of  $10 \text{ km s}^{-1}$  (*left panels*) or  $20 \text{ km s}^{-1}$  (*right panels*). The grey dots show the entire working sample, while the OC groupings are highlighted by different colours and symbols independently for both sets of linking lengths.

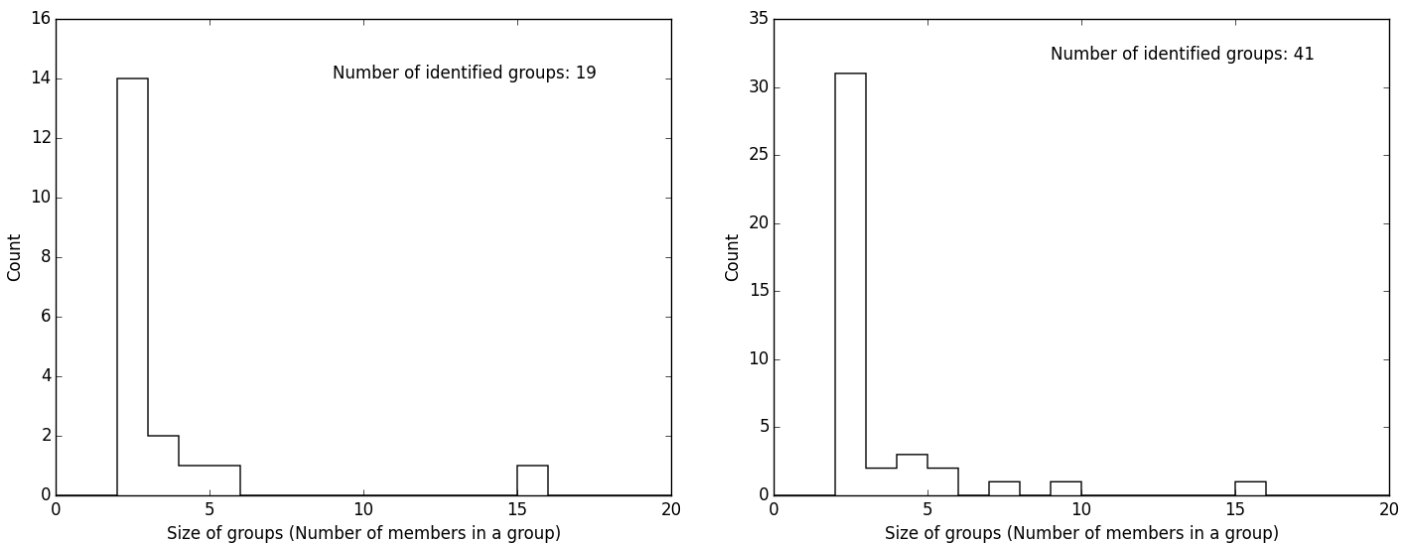


**Fig. 6.** Histograms for the size of the identified OC groupings for both sets of linking lengths: 100 pc and  $10 \text{ km s}^{-1}$  (*left panel*); 100 pc and  $20 \text{ km s}^{-1}$  (*right panel*).

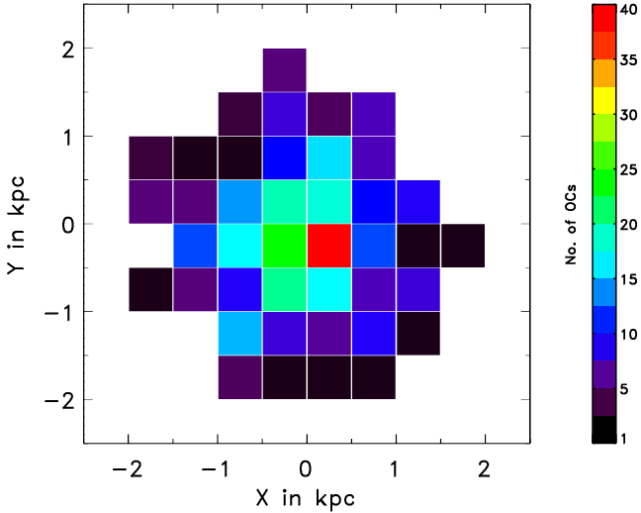


**Fig. 7.** 2D-histogram illustrating the density distribution of our working sample in the  $XY$ -plane within 1.8 kpc.

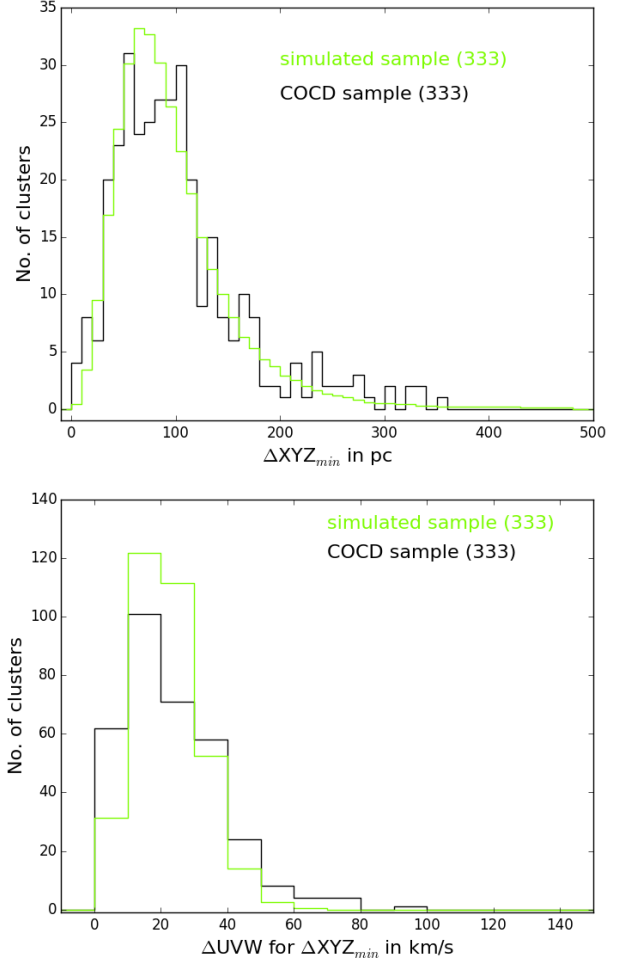
our working sample decreased to 333 OCs, defining the size of the simulated sample for better comparison.

For consistency, we applied the same FoF-like algorithm as applied to our working sample for the group identification in the simulated data with linking lengths of either 100 pc and 10 km s<sup>-1</sup> or 100 pc and 20 km s<sup>-1</sup>. To draw statistically robust conclusions on the significance of the identified structures, we compared the actual COCD results to averaged distributions for the parameters and resulting distributions for the number and size of detected groupings obtained from 1000 realisations of the Monte Carlo simulations.

As input distributions for the  $XYZ$ -coordinates and  $UVW$ -velocities for the simulated samples, we assumed that the randomised data follow the same distribution as our actual working sample. The COCD clusters are mainly located in or near the Galactic plane, which allowed us to consider the  $Z$  component of the 3D-position to be independent. In the  $XY$ -plane, we used a 2D-histogram to describe the density profile, as displayed in Fig. 7. The 2D-histogram was generated from our working sample with a bin size of 500 pc. In  $Z$ , we fitted a sech-profile to the corresponding histogram in our working sample with a bin size of 100 pc. These bin sizes were chosen to include a reasonable number of clusters in each bin so as to ensure that the potential groupings were well within one bin and not artificially induced.

For the velocity components, we assumed Gaussian profiles and fitted those to the cumulative distribution functions in our working sample to be independent of bin size and to ensure that the structure in velocity space is averaged out as well. Hereafter, this simulation is abbreviated to MC<sub>Data</sub>.

As expected, the averaged parameter distributions (individually for the  $XYZ$ -coordinates and  $UVW$ -velocities) from 1000 realisations of the MC<sub>Data</sub> show very good agreement with the corresponding distributions in our COCD working sample. Also, the averaged distributions for the spatial separations and velocity differences of the nearest neighbours in  $XYZ$ -space agree relatively well between the randomised and our working sample (see Fig. 8). Both aspects verify that the randomised samples actually represent our working sample and that we can draw reliable conclusions on the significance of the proposed structures in the Galactic OC population.



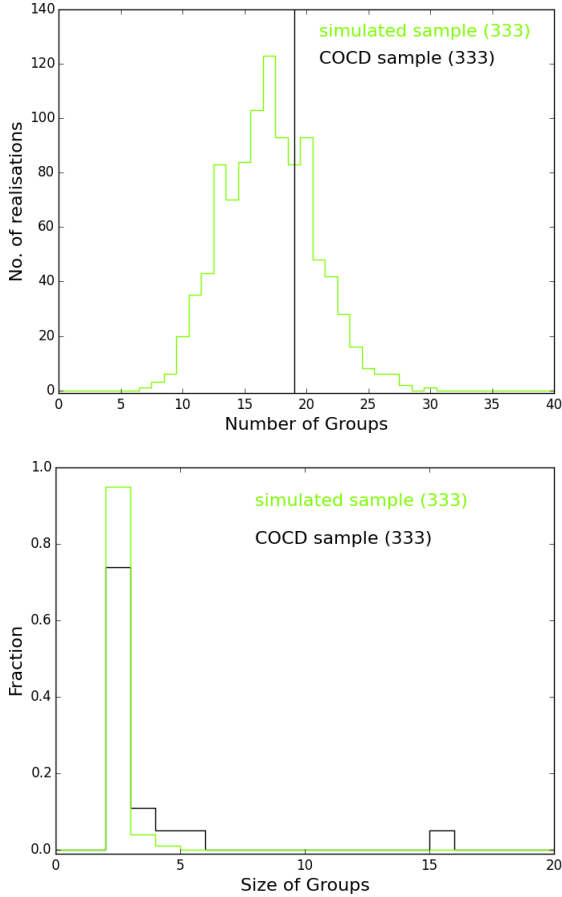
**Fig. 8.** Comparison of the distributions for the spatial separation (*upper panel*) and velocity difference (*lower panel*) of the nearest neighbours in  $XYZ$ -space. The green histograms are averaged for 1000 realisations of the MC<sub>Data</sub>. The black histograms correspond to the results from our working sample.

Figure 9 shows the histograms for the number and size of the found groupings in 1000 realisations of the MC<sub>Data</sub>. The value for the number of identified groupings in our working sample is well covered by the distribution for 1000 realisations of the MC<sub>Data</sub>. The size of the detected groupings in the real and simulated sample, on the other hand, shows a discrepancy. Though both samples tend to contain primarily pairs, the simulated samples produced no groups with more than three members. The MC<sub>Data</sub> for the second set of linking lengths (100 pc and 20 km s<sup>-1</sup>) provide similar results.

In consequence, only the complex and possibly some of the larger groups are likely to be real, while the majority of detected pairs are relatively random alignments. However, distinguishing real pairs from chance alignments is challenging, but can be achieved through an age analysis of each potential pair or smaller group. In the following section, we illustrate the idea both in general and for the found complex, which is of particular interest as it covers exactly the same members for both sets of linking lengths.

### 3.3. Characterisation of the found OC groupings

The mean parameters for the identified potential OC groupings are listed in Table B.1 for the first set of linking lengths (100 pc



**Fig. 9.** Comparison of the histograms for the number (*upper panel*) and size (*lower panel*) of the identified OC groupings for linking lengths of 100 pc and  $10 \text{ km s}^{-1}$ . The green histograms are averaged for 1000 realisations of the  $\text{MC}_{\text{Data}}$ . The black histograms correspond to the results from our working sample.

and  $10 \text{ km s}^{-1}$ ), including  $XYZ$ -coordinates,  $UVW$ -velocities, distances and ages. Mean metallicities are not included, because  $[M/H]$  values were not available for the majority of the clusters in groupings. The averaged values and the uncertainties in Table B.1 were computed as simple mean and standard deviations based on the values for the members.

One approach to evaluate the connection between OC groupings and star formation is to check the typical separations of the nearest neighbours in the young and old cluster population. Fig. 10 illustrates this comparison for the entire COCD (*upper panel*) and the recently provided more extensive catalogue for the Milky Way global survey of star clusters (MWSC; Kharchenko et al. 2013) within its completeness limit of 1.8 kpc (*lower panel*), which was used as a reference sample in this case. In the COCD, the young cluster population has ages below 20 Myr and the old population has ages above 400 Myr, while in the MWSC the young cluster population has ages below 50 Myr and the old population has ages above 700 Myr. There are two reasons for the choice of different interval margins used to extract the young and old cluster population in the COCD and the MWSC. Firstly, because the MWSC is a far more extensive Galactic cluster catalogue than the COCD, and secondly, because we wanted a similar sample size for the young and old populations in either catalogue and between the catalogues (145 OCs in COCD and approximately 195 OCs in the MWSC).

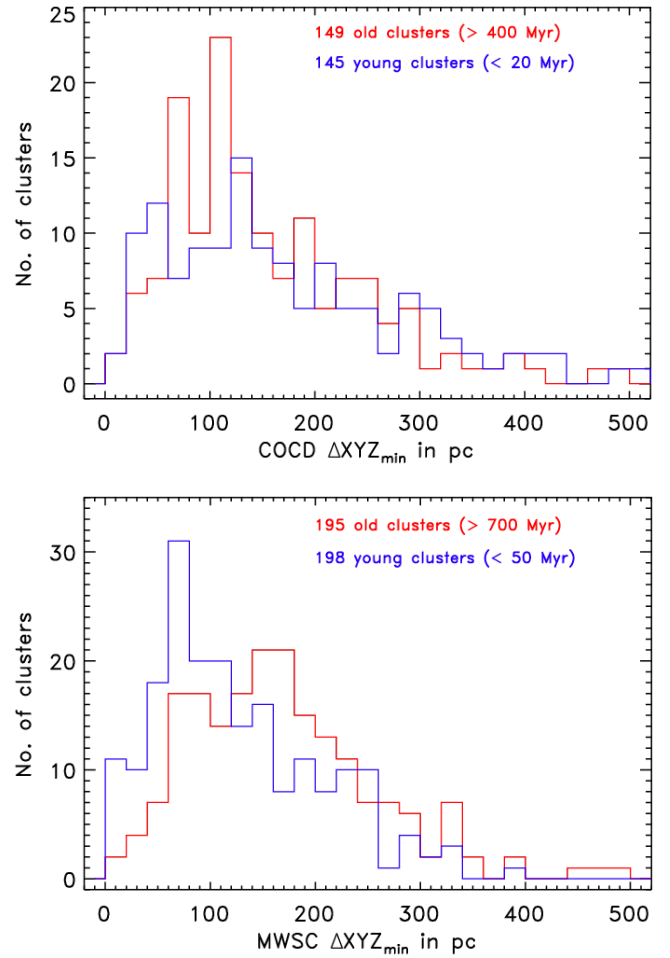


**Fig. 10.** Comparison of the spatial separation histograms of the nearest neighbours in coordinate space between the young (blue) and old (red) Galactic OC population in the entire COCD (*upper panel*; young  $< 20 \text{ Myr}$ , old  $> 400 \text{ Myr}$ ) and the MWSC within its completeness limit of 1.8 kpc (*lower panel*; young  $< 50 \text{ Myr}$ , old  $> 700 \text{ Myr}$ ).

For the young cluster population in the COCD, the distribution of the spatial separation of the nearest neighbours peaks at approximately 50 pc and 130 pc, while for the old clusters the distribution peaks at approximately 70 pc and 110 pc. In the MWSC the distribution for the spatial separation of the nearest neighbours peaks at approximately 70 pc for the young clusters and at approximately 170 for the old clusters. The double feature in the spatial separation distributions for the COCD sample may be caused by the smaller sample size affecting the statistics. In the MWSC sample, the young cluster population shows a higher density than the old cluster population, which supports the hypothesis that OC groupings most likely originate from a common molecular cloud and that clusters also form in groups. Moreover, this difference indicates that the lifetime of OC groupings might be comparable to the typical lifetime of OCs and is most likely affected by the high infant mortality in the Galactic OC population.

In the identification process, it was already indicated that all groupings detected with the first set of linking lengths (100 pc and  $10 \text{ km s}^{-1}$ ) are located within approximately 1 kpc, and the numbers in Table B.1 verify this finding. The vast majority of the detected OC groupings are actually located even within the stated completeness limit of the COCD (850 pc; Piskunov et al. 2006) and only three groupings are more distant than 1 kpc. On



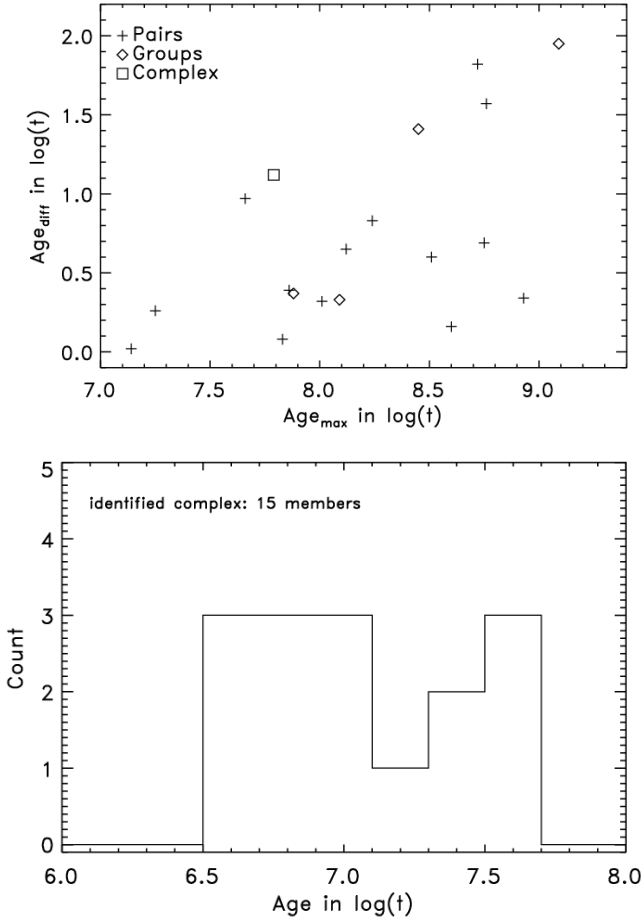


**Fig. 11.** *Upper panel:* relation between maximum age difference for the detected OC groupings and the age of its oldest member (with linking lengths 100 pc and 10 km s<sup>-1</sup>). *Lower panel:* histogram for the age distribution in the detected OC complex.

the other hand, with the second set of linking lengths (100 pc and 20 km s<sup>-1</sup>), OC groupings are also detected at larger distances (see upper panels of Fig. 5). We think that this effect is likely due to increasing tangential velocity errors with distance.

The logarithmic ages of the found OC groupings show a spread of typically below 0.5 dex, but in some cases, the spread reaches values above 1 dex (see upper panel of Fig. 11). Compared to the typical uncertainties of the COCD cluster ages of 0.2–0.25 dex, this indicates a substantial age difference within the found potential OC groupings. Nevertheless, these age differences within the potential groupings can help to distinguish between genuine groupings and chance alignments. As indicated by the higher density of the young cluster population compared to the old population (see Fig. 10), it is more likely that OC groupings originate from a common molecular cloud than that they are formed through capture. This argumentation puts certain constraints on the possible age spread for genuine OC groupings. After a few tens of millions of years, no gas is left in the vicinity of the previous maternal molecular cloud to build up stars and clusters. Thus, the age spread within real OC groupings should not exceed a few tens of millions of years. For the young candidates (average age  $\leq 100$  Myr) the spread should be within or comparable to the age uncertainties listed in the COCD (0.2–0.25 dex), while for older group candidates the spread should be well below the given uncertainties and cannot be evaluated reliably here.

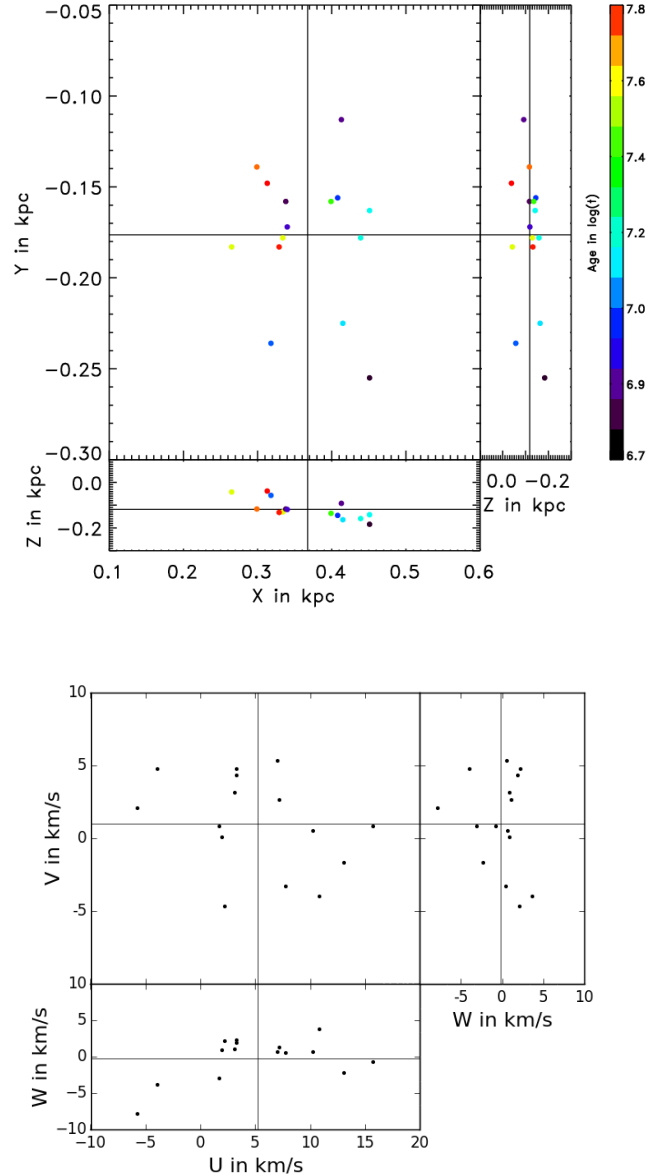


**Fig. 12.** Parameter distributions for the members of the found OC complex. *Upper panel:* spatial distribution with the age colour coded. *Lower panel:* velocity distribution. The solid lines show the averaged values for the OC complex.

Interestingly, the complex shows a rather narrow age spread as visualised in the lower panel of Fig. 11. The ages of the complex members cover a range  $\log t = 6.67\text{--}7.79$ , which corresponds to linear ages of 4.7–61.7 Myr and is comparable to the time scale of a sequential star-forming event. When looking at the spatial distribution colour-coded with age (upper panel of Fig. 12), our complex does not show a clear spatial dependence on age, as would be expected from a sequential star-formation event triggered through, for example, a supernova shock wave initiating the formation of new clusters. Such a scenario was described by Elmegreen & Lada (1977). However, if we assume multiple clusters forming initially and then triggering further cluster formation by supernova shock waves, this explains the random spatial distribution with age. If the cloud is large enough, several such triggered cluster formation events can take place sequentially over a few tens of millions of years.

Since the found complex is likely to be genuine, it is only reasonable to take a closer look at its characteristics. The

distributions in coordinate and velocity space are displayed in Fig. 12. For both sets of linking lengths (100 pc and either  $10 \text{ km s}^{-1}$  or  $20 \text{ km s}^{-1}$ ) the complex was recovered with exactly the same members, which again verifies that the complex is real. In coordinate space, the complex is very tight, covering approximately 200 pc in diameter, and in velocity space the total spread is approximately  $20\text{--}30 \text{ km s}^{-1}$ . The metallicity distribution could not be assessed, since currently only one cluster in the complex has a measured metallicity, which is supersolar ( $[M/H] = 0.14 \text{ dex}$ ). This can be suspected due to the young age of the complex.

### 3.3.1. Comparison with the literature

In addition to the characterisation of the identified OC groupings, we compared our results to the pairs, groups and complexes published in the literature (de la Fuente Marcos & de la Fuente Marcos 2009b; Piskunov et al. 2006). First, we considered the groups and complexes provided by Piskunov et al. (2006), which were identified based on spatial proximity and common tangential velocities. We present a positional comparison in the  $XY$ -plane in Fig. 13.

For the Gould-Belt complex (OCC1) from Piskunov et al. (2006) we find counterparts in our sample, namely the complex and a few groups and pairs, which shows that the third dimension in velocity space holds additional information and should not be neglected for the identification of structures in the OC population. Since the OCC1 is also referred to as the Gould-Belt complex, we compared some of the characteristics of our complex with the parameters published for the Gould Belt. For the complex, we determined an age range of approximately  $5\text{--}60 \text{ Myr}$  for its members. It is located at a distance of  $320\text{--}550 \text{ pc}$  and shows an inclination angle towards the Galactic plane of  $17\text{--}28^\circ$ . Torra et al. (2000) found that the Gould Belt is an elliptical structure of stars with ages between 30 and 60 Myr within distances of  $400\text{--}600 \text{ pc}$  and inclined towards the Galactic plane by an angle of  $16\text{--}22^\circ$ . Similar parameters are summarised in the review by Bobylev (2014) and because of the good agreement between our values for the age range, distance and inclination of our complex and those found in the literature for the Gould Belt, we conclude that the complex we detect is part of the Gould Belt structure.

For the OCC2, the Perseus-Auriga group and the Hyades group, we did not find counterparts among our OC groupings. The main reason for this discrepancy is that the majority of the members in the OCC2 and the two groups are not equipped with RV data and were therefore simply not included in our working sample. The missing RV data are indicated by the grey squares not associated by a black dot. For the OCC1 on the other hand, all members are provided with RV information, so there was a higher probability to find counterparts in our working sample.

Nevertheless, verification of the OCC1 indicated that the OCC2 and the two groups may also be real, though possibly split up into smaller groupings. Our OC groupings containing or overlapping with members of the OC complexes and groups of Piskunov et al. (2006) are summarised in Table 1, where the COCD numbers serve as guidance in the column-wise comparison. In particular, one can see that a large number of members in the Piskunov et al. (2006) complexes with high membership probability are recovered by our findings, which supports the existence of such structures in our Galaxy.

Secondly, we evaluated the pairs identified by de la Fuente Marcos & de la Fuente Marcos (2009b) by considering spatial proximity only. Their sample shows a relatively

large overlap with our sample: approximately 77% of the clusters provided by de la Fuente Marcos & de la Fuente Marcos (2009b) were present in the COCD, while only 49% of their clusters were included in our working sample. Only 15 clusters resided in any of our OC groupings, which corresponds to 39% of the common sample.

In their Table 1, de la Fuente Marcos & de la Fuente Marcos (2009b) list 34 OC pairs extracted from the WEBDA online compilation and in their Table 2, they provide 27 pairs selected from the DAML, with a significant overlap. In Table 2, we show which of our detected OC groupings at least partly overlap with the OC pairs found by de la Fuente Marcos & de la Fuente Marcos (2009b), where the cluster names can be compared. From their two tables, we found approximately one third of their pairs among our OC groupings, four of them being part of our complex. In some cases, the pairs in common are identical, whereas in others, there is only one mutual member. On the one hand, this is because only half of their clusters were included in our working sample. On the other hand, they based their identification solely on spatial proximity with a rather stringent separation criterion of 30 pc, whereas in this work, the spatial separation criterion was more relaxed (100 pc), but complemented by 3D-velocities.

For both literature samples of OC pairs, groups and complexes (de la Fuente Marcos & de la Fuente Marcos 2009b; Piskunov et al. 2006), structures are verified through our working sample, though some only partly because of incompleteness of available information, as well as of the cluster sample itself. Moreover, some of the detected OC groupings might not be genuine. However, the common pairs, groups and complexes strengthen the statement that there are overdensities in the Galactic OC population. Future investigations will reveal more details on these structures and the role they play in star formation and evolution processes in the Milky Way, as well as dynamics, structures and evolution of spiral galaxies.

## 4. Discussion and outlook

This work aimed at the identification and verification of structures in the Galactic OC population. We used the COCD as a suitable data set, since it was the most extensive homogeneous OC catalogue available. Additional RV data were obtained from RAVE and other RV catalogues<sup>3</sup>. We generated a subsample of 432 OCs out of the 650 clusters in the COCD with available 6D phase-space information.

For the identification of OC groupings, we applied an adapted FoF algorithm, as used in cosmology, in coordinate and velocity space, with linking lengths of 100 pc and  $10\text{--}20 \text{ km s}^{-1}$ . For the lower limit of the velocity linking length ( $10 \text{ km s}^{-1}$ ), we identified 19 OC groupings; 14 pairs, 4 groups of 3 to 5 members and 1 complex with 15 members, while for the upper limit ( $20 \text{ km s}^{-1}$ ) we found 41 potential OC groupings, comprising 31 pairs, 9 groups of 3 to 9 members and 1 complex with the same 15 members as identified for the lower limit. The detected OC complex is most likely part of the Gould Belt structure.

Although the choice of the linking lengths was based on reasonable criteria, it is, to a certain degree, arbitrary, and further verification of the identified structures was performed through Monte Carlo simulations exploring randomised samples, generated from the overall parameter distributions of our working sample. These simulations revealed that the larger groups and the complex are most likely genuine, while the pairs are more

<sup>3</sup> For details see Paper I.

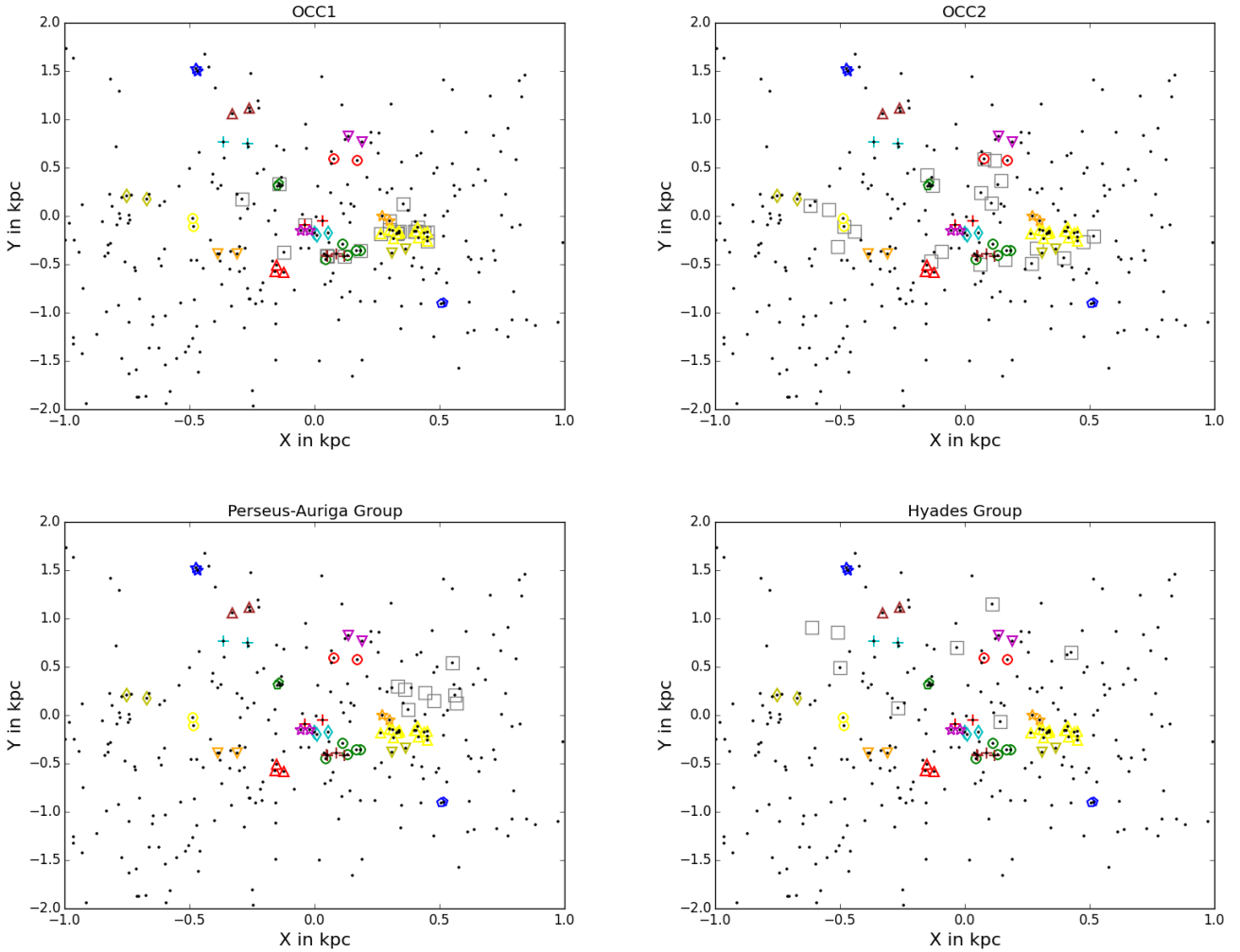


**Fig. 13.** Spatial comparison in the XY-plane of our detected OC groupings, highlighted with the same colours and symbols as in the *left panel* of Fig. 5, with the groups and complexes proposed by Piskunov et al. (2006). Black dots show COCD clusters with RV data, while grey squares indicate the members of the OCC1 and OCC2 (*upper panels*), as well as the members of the Perseus-Auriga and Hyades group (*lower panels*).

likely to be chance alignments. We have not attempted to test the success rate of the FoF method with simulated OC pairs, groups and complexes because the real spatial separations and internal velocity differences of physical cluster groupings are still unknown. Moreover, the uncertainties of currently determined OC distances and space velocities are relatively large and would probably play the dominating role in an evaluation of FoF with different linking lengths.

Our detected groups and in particular the complex may provide a hint of OC groupings originating from a common molecular cloud and forming in one, possibly sequential, star-formation event. A comparison of our findings with the pairs, groups and complexes proposed by Piskunov et al. (2006) and de la Fuente Marcos & de la Fuente Marcos (2009b) resulted in partial overlap, which fits in with a picture where OCs can form in a clustered mode. We could not recover or verify all of the OC groupings from the literature, mainly because these literature studies neglected RV data, which were essential for our investigation. It is also possible that many of the proposed groupings in the literature were not recovered because they are not real.

The cluster sample utilised in this work was homogeneous but highly incomplete, and many OC data are still uncertain with respect to distances, proper motions, membership of individual stars or missing (RVs), which allowed us to only take a first step

towards investigating OC groupings in the Milky Way. There are also systematic differences, in the distances and ages of OCs, for example, obtained from different OC surveys (Netopil et al. 2015). For example, the very famous OC pair *h*- and  $\chi$ -Persei (NGC 869 and NGC 884; Currie et al. 2010) was not recovered in our working sample, although for both clusters, RV data were available. A closer look at their COCD parameters revealed that the distance discrepancy of almost 300 pc was the main reason. In the MWSC catalogue, containing approximately 3000 stellar associations (open and globular clusters in the Milky Way) the measured distance difference between *h*- and  $\chi$ -Persei is reduced to approximately 40 pc, which would allow an identification of this OC pair with our method. Compared to the COCD, the MWSC is based on many more and fainter stars, but relies on less-accurate proper motion data and near-infrared instead of optical photometry. For approximately 1000 of the MWSC objects RVs were provided, which would significantly extend our work sample.

Another recently discovered Galactic OC binary is NGC 5617 and Trumpler 22 (De Silva et al. 2015a) with a mean age of approximately 70 Myr and similar RVs of  $-38.63$  and  $-38.46$  km s $^{-1}$ , respectively. The determined values for the mean metallicities of both clusters were  $-0.18$  and  $-0.17$  dex for NGC 5617 and Trumpler 22, respectively. We could not identify

**Table 1.** Overlap (comparing COCD numbers and names) of our detected OC groupings with the OC groups and complexes proposed by Piskunov et al. (2006) given with their membership probabilities.

Piskunov et al. (2006)			This work			Piskunov et al. (2006)			This work		
OCC1 members			Groupings and their members			OCC2 members			Groupings and their members		
COCD	name	%	COCD	name		COCD	name	%	COCD	name	
46	IC 348	84	1	44	Alessi 13		OCC2a				
68	Collinder 65	100		204	Mamajek 1	96	Collinder 95	100	10	245	Loden 143
72	Collinder 69	100	2	61	Platais 4	141	NGC 2396	100		255	vdBH 99
73	NGC 1981	100		68	Collinder 65	144	NGC 2413	100		1058	ASCC 58
74	NGC 1976	100	3	72	Collinder 69	151	Ruprecht 27	100	11	333	Loden 915
76	NGC 1980	100		73	NGC 1981	161	Ruprecht 31	100		349	ESO 175-06
77	Collinder 70	100		74	NGC 1976	168	ESO 123-26	63			
95	NGC 2232	100		75	NGC 1977	200	Ruprecht 65	100			
126	Collinder 132	100		76	NGC 1980	246	Loden 89	100			
182	Vel OB2	100		77	Collinder 70	247	Loden 59	61			
190	vdBH 23	100		80	$\sigma$ Orionis	276	NGC 3532	65			
202	IC 2391	73		91	Platais 6	344	Loden 1194	72			
204	Mamajek 1	100		95	NGC 2232	349	ESO 175-06	63			
210	Trumpler 10	100		1016	ASCC 16	373	NGC 6124	100			
261	Alessi 5	100		1018	ASCC 18	392	NGC 6281	100			
412	IC 4665	100		1019	ASCC 19	419	NGC 6469	86			
456	Stephenson 1	100		1020	ASCC 20	422	NGC 6494	100			
1016	ASCC 16	100		1021	ASCC 21	1034	ASCC 34	100			
1018	ASCC 18	100		1024	ASCC 24	1051	ASCC 51	100			
1019	ASCC 19	100	5	126	Collinder 132	1059	ASCC 59	70			
1020	ASCC 20	100		133	Collinder 135	1083	ASCC 83	100			
1021	ASCC 21	100		136	Collinder 140		low probability				
1127	ASCC 127	68		162	NGC 2451B	245	Loden 143	59			
	low probability			183	NGC 2547	333	Loden 915	24			
75	NGC 1977	40	6	159	NGC 2451A		OCC2b				
80	$\sigma$ Orionis	5		202	IC 2391	15	Platais 2	100	19	509	NGC 7438
91	Platais 6	1		218	Platais 9	514	Stock 12	100		1115	ASCC 115
133	Collinder 135	11	8	182	Vel OB2	1101	ASCC 101	100			
136	Collinder 140	15		190	vdBH 23	1109	ASCC 109	100			
159	NGC 2451A	36		210	Trumpler 10	1115	ASCC 115	100			
162	NGC 2451B	19		1048	ASCC 48	1123	ASCC 123	100			
216	Platais 8	27	9	216	Platais 8	1124	ASCC 124	100			
259	IC 2602	13		259	IC 2602						
			14	456	Stephenson 1						
				1100	ASCC 100						
Perseus-Auriga Group			Groupings and their members			Hyades Moving Group			Groupings and their members		
COCD	name		COCD	name		COCD	name		COCD	name	
37	NGC 1027					13	Alessi 1				
40	Trumpler 3					201	Praesepe				
43	King 6					459	NGC 6738				
52	NGC 1582					461	NGC 6793				
55	Alessi 2					462	NGC 6800				
81	Stock 10					494	NGC 6991				
1012	ASCC 12					502	NGC 7209				
1023	ASCC 23					1099	ASCC 99				

**Notes.** OCC2a and OCC2b are subgroups of the OCC2 structure from Piskunov et al. (2006), divided by the line along  $l \approx 15^\circ$  and  $l \approx 195^\circ$ .

this new OC pair, because both clusters were not included in our working sample due to missing RV data when we conducted our analysis. In the MWSC, the cluster NGC 5617 is provided with an RV value, while Trumpler 22 is not. However, through including additional RV data and considering the results from (De Silva et al. 2015a), this recently detected cluster pair might be confirmed with our criteria.

The parameters of previously identified OCs are not only being improved with time, but the existence of some OCs may

also be in doubt. Netopil et al. (2015) estimated that OC surveys, which, like the MWSC, used near-infrared photometry, probably contain more than 20% problematic OCs. The well known cluster Loden 1 was recently discovered to not be a cluster at all by Han et al. (2016). Thus, with updated information on the stars in OC fields, it is recommended to also check the membership selection before investigating structures and to ensure using only real objects with accurate parameters. Note that Loden 1 was included with very different parameters in the COCD and MWSC.

**Table 2.** Overlap (comparing cluster names) of our detected OC groupings with the OC pairs proposed by de la Fuente Marcos & de la Fuente Marcos (2009b) in their Tables 1 and 2.

This work			de la Fuente Marcos & de la Fuente Marcos (2009b)			
Number of OC grouping	COCD number	Cluster name	Table 1		Table 2	
			Group number	Cluster name	Group number	Cluster name
1	44	Alessi 13			1	Mamajek 1 Feigelson 1
	204	Mamajek 1				
2	61	Platais 4				
	68	Collinder 65				
3	72	Collinder 69	2	Collinder 70	3	Collinder 70
	73	NGC 1981				
	74	NGC 1976	3	NGC 1976	4	$\sigma$ Orionis NGC 1976
	75	NGC 1977				
	76	NGC 1980	4	ASCC 20	5	ASCC 20
	77	Collinder 70				
	80	$\sigma$ Orionis	6	ASCC 21	7	ASCC 21
	91	Platais 6				
	95	NGC 2232				
	1016	ASCC 16				
	1018	ASCC 18				
	1019	ASCC 19				
	1020	ASCC 20				
	1021	ASCC 21				
1024	ASCC 24					
4	125	Alessi 21				
	147	NGC 2422				
5	126	Collinder 132				
	133	Collinder 135				
	136	Collinder 140				
	162	NGC 2451B				
	183	NGC 2547				
6	159	NGC 2451A				
	202	IC 2391				
	218	Platais 9				
7	163	NGC 2447	21	NGC 2447 NGC 2448	15	NGC 2447 NGC 2448
	164	NGC 2448				
8	182	Vel OB2				
	190	vdBergh-Hagen 23				
	210	Trumpler 10				
	1048	ASCC 48				
9	216	Platais 8				
	259	IC 2602				
10	245	Loden 143				
	255	vdBergh-Hagen 99				
	1058	ASCC 58				
11	333	Loden 915				
	349	ESO 175-06				
12	392	NGC 6281	5	NGC 6405 ASCC 90	6	NGC 6405 ASCC 90
	408	NGC 6405				
13	455	Collinder 394				
	457	NGC 6716				
14	456	Stephenson 1	1	ASCC 100 ASCC 101	2	ASCC 100 ASCC 101
	1100	ASCC 100				
15	466	Turner 9				
	1110	ASCC 110				
16	476	NGC 6871	30	NGC 6871 Biurakan 1		
	477	Biurakan 1				
17	478	Biurakan 2	22	Ruprecht 172 Biurakan 2	17	Ruprecht 172 Biurakan 2
	488	NGC 6913				
18	500	IC 1396				
	501	NGC 7160				
19	509	NGC 7438				
	1115	ASCC 115				

This example shows that the MWSC results are not necessarily more reliable than those of the COCD.

Since the MWSC was only partly cross-matched with RAVE, further RV and metallicity information can be obtained from

redoing this cross-match for members of all MWSC clusters. Although SDSS data were used in the MWSC, exploring the Apache Point Observatory Galactic Evolution Experiment (APOGEE; Allende Prieto et al. 2008) survey data within the SDSS (Ahn et al. 2012) for additional information will reveal further details on OC groupings and their environment, in particular because of the dedicated OC project within APOGEE focusing on chemical information.

Both the COCD and the MWSC are catalogues of clusters that are mainly visible in the optical. Although the latter provides 2MASS data and is slightly extended towards the infrared, still large regions are apparently obscured by dust and gas clouds, as shown by a brief check. To include further very young clusters (<10 Myr), still being embedded in the gas of the molecular cloud they formed in, and rather distant systems being obscured by dust clouds in the line of sight, the MWSC can be further extended to the Infrared by including the results from the cluster project within the Visible and Infrared Survey Telescope for Astronomy (VISTA; Sutherland et al. 2015) Variables in the Via Lactea survey (VVV; Borissova et al. 2011; Chené et al. 2012, 2013; Ramírez Alegría et al. 2014).

Moreover, available data from the *Gaia*-ESO survey (Gilmore et al. 2012), along with the upcoming data from *Gaia* (Gaia Collaboration 2016) and the planned complementary spectroscopic instruments 4MOST (4m Multi Object Spectroscopic Telescope; de Jong et al. 2012; Caffau et al. 2013; Depagne 2015) and WEAVE (*William Herschel* telescope Enhanced Area Velocity Explorer; Dalton et al. 2012, 2014), will further extend the RV, metallicity and abundance data available for OC members. The significant improvement of the chemical information will enable a first attempt on studying the environmental dependency of the formation and characteristics of OC groupings. The data can be further complemented by published results on individual clusters when homogenised to a common reference frame, where necessary.

In particular, *Gaia* will improve the astrometric information and membership selection on OCs. The *Gaia Tycho* astrometric solution (TGAS) data published in the first *Gaia* data release (Lindegren et al. 2016) provide improved proper motions and, for the first time, parallaxes for the majority of the stars used in the COCD survey. The TGAS data will definitely lead to changes in the membership of individual stars and in the mean parameters of the OCs in the COCD sample. These changes and improvements are beyond the scope of this paper and will be presented elsewhere (Kharchenko et al., in prep.).

Regarding the metallicity, the dedicated APOGEE cluster project and the Galah survey (De Silva et al. 2015b), which focused on chemical tagging to identify cluster members, are of particular interest. These surveys allow a detailed chemical investigation of the identified OC pairs, groups and complexes, based on homogeneous chemical information. However, this will be subject to future studies.

In addition to extending the data set, we recommend using a different search procedure than a simple adaption of the FoF algorithm in 6D. The main challenge with the FoF algorithm is that one has to predefine the linking lengths based on prior assumptions on the structure searched for. An alternative is to use density profiles for the clusters. Groupings are then identified through searching for intersecting profiles in coordinate and velocity space.

A more detailed description and characterisation of OC groupings based on a more complete and accurate data sample will open up the opportunity to better understand star formation and structures in the Milky Way. They can be used as tracers

for the fragmentation in giant molecular clouds to improve the simulations for star and cluster formation. Many OC simulations on internal processes consider them as isolated systems only affected by Galactic forces. The verification that OCs tend to form in groups leads to rethinking this simulation approach and a detailed characterisation of these groupings helps to put constraints on the effects induced by overdensities in the Galactic OC population. Furthermore, triggered star formation can be investigated from a different point of view through considering a sequential formation of members in an OC grouping.

*Acknowledgements.* We thank the anonymous referee for a prompt report that helped us improve the paper. This work was supported by Sonderforschungsbereich SFB 881 “The Milky Way System” (subproject B5) of the German Research Foundation (DFG), and 16-52-12027 for RFBR. Funding for RAVE has been provided by: the Australian Astronomical Observatory; the Leibniz-Institut für Astrophysik Potsdam (AIP); the Australian National University; the Australian Research Council; the French National Research Agency; the German Research Foundation; the European Research Council (ERC-StG 240271 Galactic); the Istituto Nazionale di Astrofisica at Padova; The Johns Hopkins University; the National Science Foundation of the USA (AST-0908326); the W. M. Keck foundation; the Macquarie University; the Netherlands Research School for Astronomy; the Natural Sciences and Engineering Research Council of Canada; the Slovenian Research Agency; the Swiss National Science Foundation; the Science & Technology Facilities Council of the UK; Opticon; Strasbourg Observatory; and the Universities of Groningen, Heidelberg and Sydney. The RAVE web site is at <http://www.rave-survey.org>

## References

- Ahn, C. P., Alexandroff, R., Allende Prieto, C., et al. 2012, *ApJS*, 203, 21  
 Allende Prieto, C., Majewski, S. R., Schiavon, R., et al. 2008, *Astron. Nachr.*, 329, 1018  
 Bate, M. R. 2009, *MNRAS*, 392, 590  
 Bate, M. R. 2012, *MNRAS*, 419, 3115  
 Bobylev, V. V. 2014, *Astrophysics*, 57, 583  
 Bonatto, C., & Bica, E. 2010, *MNRAS*, 403, 996  
 Borissova, J., Kurtev, R., Peñalosa, F., et al. 2011, in *Rev. Mex. Astron. Astrofis. Conf. Ser.*, 40, 267  
 Caffau, E., Koch, A., Sbordone, L., et al. 2013, *Astron. Nachr.*, 334, 197  
 Calzetti, D., Lee, J. C., Sabbi, E., et al. 2015, *AJ*, 149, 51  
 Chené, A.-N., Borissova, J., Clarke, J. R. A., et al. 2012, *A&A*, 545, A54  
 Chené, A.-N., Borissova, J., Bonatto, C., et al. 2013, *A&A*, 549, A98  
 Conrad, C., Scholz, R.-D., Kharchenko, N. V., et al. 2014, *A&A*, 562, A54  
 Cottaar, M., Covey, K. R., Meyer, M. R., et al. 2014, *ApJ*, 794, 125  
 Currie, T., Hernandez, J., Irwin, J., et al. 2010, *ApJS*, 186, 191  
 Dalton, G., Trager, S. C., Abrams, D. C., et al. 2012, in *Ground-based and Airborne Instrumentation for Astronomy IV*, *Proc. SPIE*, 8446, 84460  
 Dalton, G., Trager, S., Abrams, D. C., et al. 2014, in *Ground-based and Airborne Instrumentation for Astronomy V*, *Proc. SPIE*, 9147, 91470  
 de Jong, R. S., Bellido-Tirado, O., Chiappini, C., et al. 2012, in *Ground-based and Airborne Instrumentation for Astronomy IV*, *Proc. SPIE*, 8446, 84460  
 de la Fuente Marcos, R., & de la Fuente Marcos, C. 2009a, *New Astron.*, 14, 180  
 de la Fuente Marcos, R., & de la Fuente Marcos, C. 2009b, *A&A*, 500, L13  
 de la Fuente Marcos, R., & de la Fuente Marcos, C. 2009c, *ApJ*, 700, 436  
 De Silva, G. M., Carraro, G., D’Orazi, V., et al. 2015a, *MNRAS*, 453, 106  
 De Silva, G. M., Freeman, K. C., Bland-Hawthorn, J., et al. 2015b, *MNRAS*, 449, 2604  
 Demiański, M., & Doroshkevich, A. G. 2014, *MNRAS*, 439, 179  
 Depagne, É. 2015, *Asteroseismology of Stellar Populations in the Milky Way* (Switzerland: Springer International Publishing), *Astrophys. Space Sci. Proc.*, 39, 147  
 Dias, W. S., Alessi, B. S., Moitinho, A., & Lépine, J. R. D. 2002, *A&A*, 389, 871  
 Dieball, A., Müller, H., & Grebel, E. K. 2002, *A&A*, 391, 547  
 Efremov, Y. N. 2010, *MNRAS*, 405, 1531  
 Elias, F., Alfaro, E. J., & Cabrera-Caño, J. 2009, *MNRAS*, 397, 2  
 Elmegreen, B. G. 2009, *Ap&SS*, 324, 83  
 Elmegreen, B. G. 2011, in *EAS Publications Series*, Vol. 51, *EAS Pub. Ser.*, eds. C. Charbonnel, & T. Montmerle, 31  
 Elmegreen, B. G., & Efremov, Y. N. 1996, *ApJ*, 466, 802  
 Elmegreen, B. G., & Lada, C. J. 1977, *ApJ*, 214, 725  
 Elmegreen, D. M., Elmegreen, B. G., Adamo, A., et al. 2014, *ApJ*, 787, L15  
 Foster, J. B., Cottaar, M., Covey, K. R., et al. 2015, *ApJ*, 799, 136  
 Gaia Collaboration (Prusti, T., et al.) 2016, *A&A*, 595, A1

- Geller, M. J., & Huchra, J. P. 1983, *ApJS*, **52**, 61
- Gilmore, G., Randich, S., Asplund, M., et al. 2012, *The Messenger*, **147**, 25
- Gouliermis, D. A., Thilker, D., Elmegreen, B. G., et al. 2015, *MNRAS*, **452**, 3508
- Grasha, K., Calzetti, D., Adamo, A., et al. 2015, *ApJ*, **815**, 93
- Gusev, A. S., & Efremov, Y. N. 2013, *MNRAS*, **434**, 313
- Han, E., Curtis, J. L., & Wright, J. T. 2016, *AJ*, **152**, 7
- Huchra, J. P., & Geller, M. J. 1982, *ApJ*, **257**, 423
- Kharchenko, N. V. 2001, *Kinematika i Fizika Nebesnykh Tel.*, **17**, 409
- Kharchenko, N. V., Piskunov, A. E., Röser, S., Schilbach, E., & Scholz, R.-D. 2004, *Astron. Nachr.*, **325**, 740
- Kharchenko, N. V., Piskunov, A. E., Röser, S., Schilbach, E., & Scholz, R.-D. 2005a, *A&A*, **438**, 1163
- Kharchenko, N. V., Piskunov, A. E., Röser, S., Schilbach, E., & Scholz, R.-D. 2005b, *A&A*, **440**, 403
- Kharchenko, N. V., Scholz, R.-D., Piskunov, A. E., Röser, S., & Schilbach, E. 2007, *Astron. Nachr.*, **328**, 889
- Kharchenko, N. V., Berczik, P., Petrov, M. I., et al. 2009, *A&A*, **495**, 807
- Kharchenko, N. V., Piskunov, A. E., Schilbach, E., Röser, S., & Scholz, R.-D. 2013, *A&A*, **558**, A53
- Kordopatis, G., Gilmore, G., Steinmetz, M., et al. 2013, *AJ*, **146**, 134
- Kravtsov, A. V., & Borgani, S. 2012, *ARA&A*, **50**, 353
- Kunder, A., Kordopatis, G., Steinmetz, M., et al. 2017, *AJ*, **153**, 75
- Lada, C. J. 2006, *ApJ*, **640**, L63
- Lada, C. J., & Lada, E. A. 2003, *ARA&A*, **41**, 57
- Lindegren, L., Lammers, U., Bastian, U., et al. 2016, *A&A*, **595**, A4
- Mermilliod, J. C. 1988, *Bulletin d'Information du Centre de Données Stellaires*, **35**, 77
- Netopil, M., Paunzen, E., & Stütz, C. 2012, in *Developments of the Open Cluster Database WEBDA*, eds. A. Moitinho, & J. Alves (Berlin, Heidelberg: Springer-Verlag), 53
- Netopil, M., Paunzen, E., & Carraro, G. 2015, *A&A*, **582**, A19
- Piatti, A. E., Clariá, J. J., & Ahumada, A. V. 2010, *PASP*, **122**, 516
- Piskunov, A. E., Kharchenko, N. V., Röser, S., Schilbach, E., & Scholz, R.-D. 2006, *A&A*, **445**, 545
- Ramírez Alegría, S., Borissova, J., Chené, A. N., et al. 2014, *A&A*, **564**, L9
- Sánchez, N., Añez, N., Alfaro, E. J., & Crone Odekon, M. 2010, *ApJ*, **720**, 541
- Steinmetz, M., Zwitter, T., Siebert, A., et al. 2006, *AJ*, **132**, 1645
- Sutherland, W., Emerson, J., Dalton, G., et al. 2015, *A&A*, **575**, A25
- Torra, J., Fernández, D., & Figueras, F. 2000, *A&A*, **359**, 82